International Journal of Advanced Research in Electrical, Electronics and Instrumentation Engineering (IJAREEIE)

| e-ISSN: 2278 – 8875, p-ISSN: 2320 – 3765| www.ijareeie.com | Impact Factor: 7.122|

||Volume 9, Issue 7, July 2020||

Neural Fault-Tolerant Nonlinear Control for Uncertain Ducted Fan Engine of Thrust-Vectored Aircraft

Olivier Baraka Mushage

Associate Professor, Faculty of Applied Sciences and Technologies, Université Libre des Pays des Grands Lacs

ABSTRACT: This paper addresses the control problem of a ducted fan in thesimultaneous presence of external disturbance, actuation faults and unknown dynamics. A nonlinear fault-tolerant adaptive controller is designed, which uses some dynamic parameters and two radial basis function neural networks. The dynamic parameters are tuned online to cancel the effects caused by external disturbances, actuation failures and neural networks approximation errors. A Lyapunov's stability analysis is performed to prove that closed-loop stability of the system is guaranteed with the proposed controller. A simulation is performed to demonstrate the high performance guaranteed to the ducted fan aircraft with the proposed controller. The results obtained using this controller are compared to those obtained using a traditional sliding mode controller, in the same situation. It is demonstrated that the proposed controller leads to some very interesting results in terms of tracking accuracy and control efforts.

KEYWORDS: Ducted fan, nonlinear control, adaptive control, neural networks.

I.INTRODUCTION

Nonlinear controllers are well known to provide best results when it comes to controlling nonlinear dynamic systems, which are the majority of practical engineering systems. Among those systems, for which high performance is required, are vectored propulsion systems of modern jet aircrafts, which serve as good platform for improving important capabilities such as executing quick transition between hover, forward flight and reverse flight, as well as other aggressive manoeuvres (Fazeli Asl & Seyyed, 2017). Specifically, for those vehicles that do not require landing runway and that can be used in small environments, one of their most important parts is the ducted fun engine which is used for aircrafts like the F18-HARV, the X-31, the XV-9A or some UAVs (unmanned aerial vehicles)in vertical take-off and landing(VTOL) [2-11]. Ducted fan aircrafts are usually instable with complex aerodynamics, which makes them highly nonlinear and uncertain. Therefore, robust nonlinear controllers are needed to tackle these challenges. Several nonlinear controllers have been proposed in the literature for different types of ducted fan aircrafts.

A combination of backstepping control andfast terminal sliding mode control was considered in (Fazeli Asl & Seyyed, 2017) for controllingaducted fan engine of a thrust-vectored aircraft subject tounmatched uncertainties and external disturbances. To increasethe speed of convergence of the system states to the equilibriumpoints or to decay state errors to zero, the authors used the fast terminal slidingmode controller. The model-based predictive control of a ducted fan was addressed in (Emami & Rezaeizadeh, 2018) for attitude and trajectory tracking of a VTOL aircraft in the simultaneous presence of model uncertainties and external disturbances. The authors proposed two modified robustand adaptive model predictive controllers for tracking a predefined path in the presence of external gusts andmodel uncertainties. The design was performed by introducing two novel observers to estimate the model uncertainties andexternal disturbances, simultaneously. Authors of (Yu, Jadbabaie, & Primbs, Comparison of nonlinear control design techniques on a model of the Caltech ducted fan, 2001) designed and compared two different nonlinear control design methods for the planar model of a ducted fan engine.These methods required the Jacobian linearization of the nonlinear plant before the design of an LQR controller, and using modelpredictive control and linear parameter varying methods. Authors of (Cheng, Pei, & Li, 2020) have focused on the transition control of a ducted fan vertical take-off and landing(VTOL) unmanned aerial vehicle (UAV). A Neural-networks (NNs) based controller was used to achieve a steady transition from hover to high-speed flight while learning the system dynamics and compensating for the trackingerror between the aircraft dynamics and the desired dynamicperformance. Controller andestimation algorithms were studied in (Peddle, Jones, & Treurnicht, 2009)for an electrically powered, coaxial,counterrotating ducted fan aircraft (SLADe-surface launched aerial decoy) to operate with low-cost sensors, becomputationally efficient,robust and easily adaptable from flight test data. Successive loop closure was employed in the controllerdesign with feedback signals from linear decoupled estimators. A robust adaptive fault-tolerant controller was developed in

| e-ISSN: 2278 – 8875, p-ISSN: 2320 – 3765| www.ijareeie.com | Impact Factor: 7.122|

||Volume 9, Issue 7, July 2020||

(Wang, Xiang, Najjaran, & Xu, 2018) for a tandem coaxial ducted fan aircraft under system uncertainty, mismatched disturbance, and actuator saturation.Mismatched disturbance attenuation was ensured through a structured H-infinity controller tuned by a non-smooth optimization algorithm. In addition, an adaptive control law was proposed in order to mitigate matched system uncertaintyand actuator fault. A control strategy was studied in (Naldi, Torre, & Marconi, 2015)for a miniature ducted-fan aerial robot tosafely perform flight missions inan unknown densely populated environment.

Inspired by the above discussion, this paper focuses on the control of the planar model of a ducted fan engine under the simultaneous presence of unmatched model uncertainties, external disturbances and actuation faults like loss of effectiveness. The study considers the use of Radial Basis Function Neural-Networks (RBFNNs), to deal with the uncertain dynamics, and the use of some online tuned parameters used in the control law to tackle issues related to actuation faults, external disturbances and NNs' approximation errors simultaneously.

This paper is organized as follows. Section II presents the dynamical model of a planar ducted fan and introduces the control problem addressed in this work. Section III presents the proposed adaptive nonlinear control strategy and the stability analysis of the controlled system. In section IV, simulation results obtained using the prosed controller are presented and compared to those obtained using the traditional sliding mode control.Finally, in Section V the paper is concluded.

II.SYSTEM MODEL AND CONTROL PROBLEM STATEMENT

In this work we consider a model of the Caltech ducted fan, which is a simple planar model of the ducted fan depicted by Fig. 1, in which the stand dynamics are ignored.

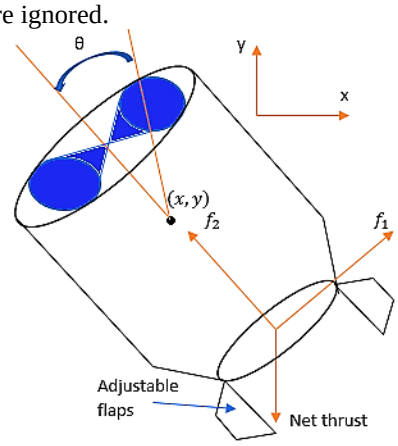

Figure 1 Planar ducted fan model

In Fig.1,(x, y, θ) denote the position and orientation of a given point located on the main axis of the fan at a distance l from the centre of mass. Two forces act on the fan;f_1, which is a force acting on the fan perpendicularly to its axis at a distance r and f_2, which is a force acting on the fan parallelly to the its axis.
Let m_x, m_y, J,$g$and $m_g$denote the inertial mass of the fan in the x and y directions, the moment of inertia, the gravitational constant, and the weight of the fan, respectively. The equation of motion can therefore be written as follows[1,12-15]:

$$\begin{cases} m_x\ddot{x} = -d\dot{x} + f_1\cos\theta - f_2\sin\theta \\ m_y\ddot{y} = -d\dot{y} + f_1\sin\theta + f_2\cos\theta - m_g g \\ J\ddot{\theta} = rf_1 \end{cases} \quad (1)$$

where d is the viscous friction coefficient used to model drag terms in the x and y directions. By redefining the inputs as $u_1 = f_1$ and $u_2 = f_2 - m_g g$, the origin is an equilibrium point of the system with zero input and equations known as the planar ducted fan equations are obtained as follows:

| e-ISSN: 2278 – 8875, p-ISSN: 2320 – 3765| www.ijareeie.com | Impact Factor: 7.122|

||Volume 9, Issue 7, July 2020||

$$\begin{cases} m_x\ddot{x} = -mg\sin\theta - d\dot{x} + u_1\cos\theta - u_2\sin\theta \\ m_y\ddot{y} = mg(\cos\theta - 1) - d\dot{y} + u_1\sin\theta + u_2\cos\theta \\ J\ddot{\theta} = ru_1 \end{cases} \quad (2)$$

Equation (2) can be rewritten in a vector form as follows:

$$\ddot{\boldsymbol{q}} = \boldsymbol{D}\dot{\boldsymbol{q}} + \boldsymbol{m} + \boldsymbol{d_f} + \boldsymbol{K_a u} \quad (3)$$

$$\ddot{\theta} = \frac{r}{J}u_1$$

where $\boldsymbol{u} = [u_1 \quad u_2]^T$, $\boldsymbol{q} = [x \quad y]^T$, $\boldsymbol{D} = \begin{bmatrix} -\frac{d}{m_x} & 0 \\ 0 & -\frac{d}{m_y} \end{bmatrix}$, $\boldsymbol{K_a} = \begin{bmatrix} \frac{\cos\theta}{m_x} & -\frac{\sin\theta}{m_x} \\ \frac{\sin\theta}{m_y} & \frac{\cos\theta}{m_y} \end{bmatrix}$, $m = \begin{bmatrix} -\frac{mg\sin\theta}{m_x} \\ \frac{mg(\cos\theta-1)}{m_y} \end{bmatrix}$ and $\boldsymbol{d_f} = \begin{bmatrix} d_{f1} \\ d_{f2} \end{bmatrix}$.

By setting $\boldsymbol{X} = [\boldsymbol{X_1} \quad \boldsymbol{X_2}]^T$, with $\boldsymbol{X_1} = \boldsymbol{q}$ and $\boldsymbol{X_2} = \dot{\boldsymbol{q}}$ the first equation ofEq. (3) becomes:

$$\begin{cases} \dot{\boldsymbol{X}}_1 = \boldsymbol{X_2} \\ \dot{\boldsymbol{X}}_2 = \boldsymbol{D}\boldsymbol{X_2} + \boldsymbol{m} + \boldsymbol{d_f} + \boldsymbol{K_a u} \\ \boldsymbol{Y} = \boldsymbol{X_1} \end{cases} \quad (4)$$

In case of actuation failure, specifically loss of effectiveness, the actuation signal applied to the system is expressed as follows:

$$\boldsymbol{u} = (1-\alpha)\boldsymbol{u_i} \quad (5)$$

where $0 \le \alpha < 1$ is the ration of the lost effectiveness and $\boldsymbol{u_i}$ is the actuator's input.
By applying Eq. (5) in the second expression of Eq. (4) we obtain

$$\dot{\boldsymbol{X}}_2 = \boldsymbol{D}\boldsymbol{X_2} + \boldsymbol{m} + \boldsymbol{K_a u_i} + \boldsymbol{\xi_f}(\boldsymbol{t}, \boldsymbol{u_i}) \quad (6)$$

where $\boldsymbol{\xi_f}(\boldsymbol{t}, \boldsymbol{u_i}) = \boldsymbol{d_f} - \boldsymbol{\alpha K_a u_i}$ is a lumped disturbance term corresponding to external disturbances and actuation faults.

In order to guarantee high performance for ducted fan aircraft, the problem consists in designing a control scheme able to force the system's output $\boldsymbol{Y} = [x \quad y]^T$ to track a given reference trajectory $\boldsymbol{Y_d} = [x_d \quad y_d]^T$ despite external disturbances, system parameters changes and actuation faults. Therefore, angle θ is not to be controlled.

III. NEURAL ADAPTIVE FAULT-TELERANT NONLINEAR CONTROLLER (NAFTNC) DESIGN

In this section, a controller is designed for the ducted fun system such that its actuator can generate a control signal $\boldsymbol{u}(\boldsymbol{t})$ that guarantees that the output $\boldsymbol{Y} = \boldsymbol{X_1} = [x \quad y]^T$ can track a given desired trajectory $\boldsymbol{Y_d} = [x_d \quad y_d]^T$ regardless of potential perturbations related to parameters changes, actuation failure and external disturbances.

Let us set

$$\boldsymbol{K_a} = \boldsymbol{M} \cdot \boldsymbol{G}(\boldsymbol{\theta}) \quad (7)$$

where $\boldsymbol{M} = \begin{bmatrix} 1/m_x & 0 \\ 0 & 1/m_y \end{bmatrix}$ and $\boldsymbol{G}(\boldsymbol{\theta}) = \begin{bmatrix} \cos\theta & -\sin\theta \\ \sin\theta & \cos\theta \end{bmatrix}$

so that Eq. (6) (with $\boldsymbol{\xi_f}(\boldsymbol{t}, \boldsymbol{u_i}) = \boldsymbol{0}$) can be rewritten as follows:

$$\boldsymbol{M^{-1}}\dot{\boldsymbol{X}}_2 = \boldsymbol{M^{-1}}(\boldsymbol{D}\boldsymbol{X_2} + \boldsymbol{m}) + \boldsymbol{G}(\boldsymbol{\theta})\boldsymbol{u_i} \quad (8)$$

Let us denote $\boldsymbol{e} = [e_x \quad e_y]^T$ the tracking error vector where $e_x = x - x_d$ and $e_y = y - y_d$ are the tracking errors on the x and y positions, respectively;thus $\boldsymbol{e} = \boldsymbol{X_1} - \boldsymbol{X_{1d}}$ and $\dot{\boldsymbol{e}} = \boldsymbol{X_2} - \dot{\boldsymbol{X}}_{\boldsymbol{1d}}$. Now let us select a filtering error vector function $\boldsymbol{s} = [s_x \quad s_y]^T$ expressed as follows:

$$\boldsymbol{M^{-1}s} = \boldsymbol{M^{-1}}\dot{\boldsymbol{e}} + \boldsymbol{M^{-1}ce} \quad (9)$$

where $\boldsymbol{c} \in \mathbb{R}^{2\times 2}$ is a diagonal matrix for which the diagonal entries are selected as $c_1 > 0$ and $c_2 > 0$.

The first time derivative of Eq. (9), where Eq. (8)is applied, yields:

| e-ISSN: 2278 – 8875, p-ISSN: 2320 – 3765| www.ijareeie.com | Impact Factor: 7.122|

||Volume 9, Issue 7, July 2020||

$$\boldsymbol{M^{-1}\dot{s} = M^{-1}\dot{X}_2 - M^{-1}\ddot{X}_{1d} + M^{-1}c\dot{e}}$$

$$= \boldsymbol{M^{-1}(DX_2 + m) + G(\theta)u_i - M^{-1}\ddot{X}_{1d} + M^{-1}c\dot{e}} \quad (10)$$

Let us define another expression of the first-time derivative of the filtered error function as follows:

$$\boldsymbol{\dot{M^{-1}}\dot{s} = -\hat{\eta}T(s) - KE(s)} \quad (11)$$

where $\boldsymbol{K} = \text{diag}(K_1, K_2)$ with $K_1 > 0,\ K_2 > 0; \boldsymbol{\hat{\eta}} = \text{diag}\left(\hat{\eta}_x(t), \hat{\eta}_y(t)\right)$ is a diagonal matrix for which entries $\hat{\eta}_j(t)$(with $j = x, y$)are computed in real time using the following expression:

$$\hat{\eta}_j(t) = \hat{\eta}_{j1}(t) + \eta_{j2}(t) \quad (12)$$

Where

$$\dot{\hat{\eta}}_{j1}(t) = \left|\hat{s}_j\right|/\gamma_{j\eta} \quad (13)$$

and

$$\eta_{j2}(t) = \rho_j\left|\hat{\varepsilon}_j\right| \quad (14)$$

with$\rho_j > 1$being an arbitrary design parameter; $\hat{\varepsilon}_j$is a dynamic parameter, which can be obtained using:

$$\dot{\hat{\varepsilon}}_j(t) = \hat{s}_j/\gamma_{\varepsilon_j} \quad (15)$$

The entries of vectors$\boldsymbol{T(s)} = \left[T_x(s_x) \quad T_y(s_y)\right]^T$and $\boldsymbol{E(s)} = \left[E_x(s_x) \quad E_y(s_y)\right]^T$are obtained using the following expressions:

$$T_j(s_j) = (e^{4s_j} - 1)/(e^{4s_j} + 1) \quad (16)$$

$$E_j(s_j) = s_j/(e^{4s_j} + 1) \quad (17)$$

By making Eq. (10) equal to Eq. (11) we deduce the control law vector as follows:

$$\boldsymbol{u_i = G(\theta)^{-1}[-f(X) - \hat{\eta}T(s) - KE(s)]} \quad (18)$$

where $\boldsymbol{f(X) = M^{-1}\left(DX_2 + m - \ddot{X}_{1d} + c\dot{e}\right)}$is a nonlinear vector function that depends on the system's parameters m_x, m_y and d. Considering that these parameters are uncertain or unknown, $\boldsymbol{f(X)}$cannot be exactly obtained such that Eq. (18) cannot be implemented in its current state. In order to tackle this issue, let us use RBFNNs to find an approximation of the unknown vector function. RBFNNsare characterized by their three layers, which are the input layer, the hidden layer, and the output layer. RBFNN have been proven able to provide good approximations of some smooth nonlinear functions on a compact set Ω using the universal approximation theorem (Lili, Yixin, Huajun, Yongchuan, & Binghua, 2018; Dongdong, Guofeng, Yunsheng, Yiming, & Yongsheng, 2018).

In this work, two RBFNNs for which the respective inputs are $\boldsymbol{x_{ex}} = [e_x \quad \dot{e}_x]^T$and $\boldsymbol{x_{ey}} = [e_y \quad \dot{e}_y]^T$, with n neurons in the hidden layer, are used to provide at their outputs the entries $\boldsymbol{\hat{f}_j(X_{ej}|\widehat{W}_j)}$ of the approximated vector function$\boldsymbol{\hat{f}(X_e|\widehat{W})} = \left[\hat{f}_x\left(\boldsymbol{X_{ex}}|\widehat{\boldsymbol{W}}_x\right) \quad \hat{f}_y\left(\boldsymbol{X_{ey}}|\widehat{\boldsymbol{W}}_y\right)\right]^T$as follows:

$$\hat{f}\left(\boldsymbol{x_{ej}}|\widehat{\boldsymbol{W}}_j\right) = \widehat{\boldsymbol{W}}_j^T\boldsymbol{h}_j\left(\boldsymbol{x_{ej}}\right) \quad (19)$$

such that$\boldsymbol{\hat{f}(X_e|\widehat{W})} = \boldsymbol{\widehat{W}^T h(X_e)}$,with$\boldsymbol{X_e} = [\boldsymbol{x_{ex}} \quad \boldsymbol{x_{ey}}]^T; \widehat{\boldsymbol{W}} = \left[\widehat{\boldsymbol{W}}_x \quad \widehat{\boldsymbol{W}}_y\right]$ where $\widehat{\boldsymbol{W}}_j^T = [W_{j1} \quad W_{j2} \quad \cdots \quad W_{jn}]$ is the$j$th estimate weighting vector for which an update rule is defined as $d\widehat{\boldsymbol{W}}_j/dt = \gamma_j^{-1}s_j\boldsymbol{h_j}\left(\boldsymbol{x_{ej}}\right)$,which corresponds to

$$\dot{\widehat{\boldsymbol{W}}} = \boldsymbol{\Gamma^{-1}h}(\boldsymbol{x_e})\boldsymbol{s^T} \quad (20)$$

with $\boldsymbol{\Gamma} = \boldsymbol{\Gamma^T} > 0 \in \mathbb{R}^{2\times2}$ and $\boldsymbol{h}(\boldsymbol{x_e}) = \left[\boldsymbol{h_x^T}(\boldsymbol{x_{ex}}) \quad \boldsymbol{h_y^T}\left(\boldsymbol{x_{ey}}\right)\right]^{\boldsymbol{T}}$ where the entries$\boldsymbol{h_j^T}\left(\boldsymbol{x_{ej}}\right) = \left[h_{j1} \quad h_{j2} \quad \cdots \quad h_{jm}\right]$ are the radial basis vector functions for which the elements are obtained using :

$$h_{1j}(\boldsymbol{x_{e1}}) = \exp\left(-\frac{\left\|\boldsymbol{x_{ej}} - \boldsymbol{\lambda_{ji}}\right\|^2}{2\beta_j^2}\right) \quad (21)$$

with $\lambda_{ji} \in \mathbb{R}^{2\times1}$ being the centric vector, $\beta_j \in \mathbb{R}$ being the base width of the radial basis functions.

| e-ISSN: 2278 – 8875, p-ISSN: 2320 – 3765| www.ijareeie.com | Impact Factor: 7.122|

||Volume 9, Issue 7, July 2020||

The differences between the neural networks' outputs and the exact nonlinear functions they approximate are expressed by:

$$\hat{\boldsymbol{f}}\left(\boldsymbol{X_e}|\widehat{\boldsymbol{W}}\right) - \boldsymbol{f}(\boldsymbol{X}) = \widetilde{\boldsymbol{W}}^{\boldsymbol{T}}\boldsymbol{h}(\boldsymbol{X_e}) - \boldsymbol{\varepsilon}(\boldsymbol{X_e})\boldsymbol{I_2} \quad (22)$$

where $\boldsymbol{I_2} \in \mathbb{R}^2$is a unit column vector, $\widetilde{\boldsymbol{W}}$is the error ofweighting matrix approximation and the RBFNN approximationerror vector is$\boldsymbol{\varepsilon}(\boldsymbol{X_e}) = \left[\varepsilon_x(\boldsymbol{x_{ex}}), \varepsilon_y\left(\boldsymbol{x_{ey}}\right)\right]^{\boldsymbol{T}}$,which is assumed bounded by an unknown constant$\mathbf{E}_{\boldsymbol{xy}}$.

Now that we have expressed the approximation of the unknown nonlinear function $\boldsymbol{f}(\boldsymbol{X})$, the control law (the NAFTNC) to be implemented is expressed as follows:

$$\boldsymbol{u_i} = \boldsymbol{G}(\boldsymbol{\theta})^{-1}\left[-\hat{\boldsymbol{f}}\left(\boldsymbol{X_e}|\widehat{\boldsymbol{W}}\right) - \hat{\boldsymbol{\eta}}\boldsymbol{T}(\boldsymbol{s}) - \boldsymbol{KE}(\boldsymbol{s})\right] \quad (23)$$

By applying Eqs. (22) and (23) in Eq. (10) (where $\boldsymbol{\xi_f}(\boldsymbol{t}, \boldsymbol{u_i}) \neq \boldsymbol{0}$) we obtain

$$\boldsymbol{M^{-1}} \cdot \dot{\boldsymbol{s}} = -\left[\widetilde{\boldsymbol{W}}^{\boldsymbol{T}}\boldsymbol{h}(\boldsymbol{X_e}) - \boldsymbol{\varepsilon}(\boldsymbol{X_e})\boldsymbol{I_6}\right] + \boldsymbol{\xi_f}(\boldsymbol{t}, \boldsymbol{u_i}) - \hat{\boldsymbol{\eta}}\boldsymbol{T}(\boldsymbol{s}) - \boldsymbol{KE}(\boldsymbol{s}) \quad (24)$$

In order to prove that with the NAFTNCexpressed by Eq. (23) the closed-loop system is stable, let us now consider the following candidate Lyapunov function:

$$V = V_1 + V_2 \quad (25)$$

with

$$V_1 = \frac{1}{2}\boldsymbol{s}^{\boldsymbol{T}}\boldsymbol{M}^{-1}\boldsymbol{s} + \frac{1}{2}\mathbf{tr}\left[\widetilde{\boldsymbol{W}}^{\boldsymbol{T}}\boldsymbol{\Gamma}\widetilde{\boldsymbol{W}}\right] \quad (26)$$

where the error on $\widehat{\boldsymbol{W}}$is defined as follows:

$$\widetilde{\boldsymbol{W}} = \widehat{\boldsymbol{W}} - \boldsymbol{W}^* \quad (27)$$

$\boldsymbol{W}^* \in \mathbb{R}^{\boldsymbol{2m\times 2}}$is the optimal weight matrix considered hereonly for analytic purpose.By considering$\hat{\boldsymbol{\eta}}_1\boldsymbol{I_2}$to be anestimationof the lumped disturbance $\boldsymbol{\xi_f}(\boldsymbol{t}, \boldsymbol{u_i})$ the approximation error is expressed as follows

$$\tilde{\boldsymbol{\eta}}_1\boldsymbol{I_6} = \hat{\boldsymbol{\eta}}_1\boldsymbol{I_6} - \boldsymbol{\xi_f}(\boldsymbol{t}, \boldsymbol{u_i}) \quad (28)$$

Not let us set

$$V_2 = \frac{1}{2}\mathbf{tr}\left[\tilde{\boldsymbol{\eta}}_1^{\boldsymbol{T}}\boldsymbol{\Gamma}_{\boldsymbol{\eta}}\tilde{\boldsymbol{\eta}}_1\right] + \frac{1}{2}\tilde{\boldsymbol{\varepsilon}}^{\boldsymbol{T}}\,\boldsymbol{\Gamma}_{\boldsymbol{\varepsilon}}\tilde{\boldsymbol{\varepsilon}} \quad (29)$$

whereis the diagonal matrix of error on parameter $\hat{\boldsymbol{\varepsilon}} \in \mathbb{R}^{\boldsymbol{2\times 2}}$(the approximate RBFNN error) is given as:

$$\tilde{\boldsymbol{\varepsilon}} = \hat{\boldsymbol{\varepsilon}} - \boldsymbol{\varepsilon}(\boldsymbol{X_e}) \quad (30)$$

By applying Eq. (27) in the first-time derivative of V_1we obtain:

$$\dot{V}_1 = \boldsymbol{s}^{\boldsymbol{T}}\boldsymbol{M}\dot{\boldsymbol{s}} + \mathrm{tr}\left[\widetilde{\boldsymbol{W}}^{\boldsymbol{T}}\boldsymbol{\Gamma}\dot{\widetilde{\boldsymbol{W}}}\right]$$

$$= \boldsymbol{s}^{\boldsymbol{T}}\boldsymbol{M}\dot{\boldsymbol{s}} + \mathrm{tr}\left[\widetilde{\boldsymbol{W}}^{\boldsymbol{T}}\boldsymbol{\Gamma}\dot{\widetilde{\boldsymbol{W}}}\right] \quad (31)$$

Let us now apply Eqs. (20) and (24) in Eq.(31) to obtain:

$$\dot{V}_1 = \boldsymbol{s}^{\boldsymbol{T}}\left\{-\left[\widetilde{\boldsymbol{W}}^{\boldsymbol{T}}\boldsymbol{h}(\boldsymbol{X_e}) - \boldsymbol{\varepsilon}(\boldsymbol{X_e})\boldsymbol{I_2}\right] + \boldsymbol{\xi_f}(\boldsymbol{t}, \boldsymbol{u_i}) - \hat{\boldsymbol{\eta}}\boldsymbol{T}(\boldsymbol{s}) - \boldsymbol{KE}(\boldsymbol{s})\right\} + \mathbf{tr}\left[\widetilde{\boldsymbol{W}}^{\boldsymbol{T}}\boldsymbol{\Gamma}\dot{\widetilde{\boldsymbol{W}}}\right]$$

$$= \mathbf{tr}\left[\widetilde{\boldsymbol{W}}^{\boldsymbol{T}}\left(\boldsymbol{\Gamma}\dot{\widetilde{\boldsymbol{W}}} - \boldsymbol{h}(\boldsymbol{X_e})\right)\boldsymbol{s}^{\boldsymbol{T}}\right] + \boldsymbol{s}^{\boldsymbol{T}}\boldsymbol{\varepsilon}(\boldsymbol{X_e})\boldsymbol{I_2} + \boldsymbol{s}^{\boldsymbol{T}}\,\boldsymbol{\xi_f}(\boldsymbol{t}, \boldsymbol{u_i}) - \boldsymbol{s}^{\boldsymbol{T}}\hat{\boldsymbol{\eta}}\boldsymbol{T}(\boldsymbol{s}) - \boldsymbol{s}^{\boldsymbol{T}}\boldsymbol{KE}(\boldsymbol{s}) \quad (32)$$

Let us now apply identities given by Eqs. (28) and (30) to the first-time derivative to Eq. (29) to obtain:

$$\dot{V}_2 = \mathbf{tr}\left[\tilde{\boldsymbol{\eta}}_1^{\boldsymbol{T}}\boldsymbol{\Gamma}_{\boldsymbol{\eta}}\dot{\tilde{\boldsymbol{\eta}}}_1\right] + \tilde{\boldsymbol{\varepsilon}}^{\boldsymbol{T}}\boldsymbol{\Gamma}_{\boldsymbol{\varepsilon}}\dot{\tilde{\boldsymbol{\varepsilon}}} = \mathbf{tr}\left[\tilde{\boldsymbol{\eta}}_1^{\boldsymbol{T}}\boldsymbol{\Gamma}_{\boldsymbol{\eta}}\dot{\hat{\boldsymbol{\eta}}}_1\right] + \tilde{\boldsymbol{\varepsilon}}^{\boldsymbol{T}}\boldsymbol{\Gamma}_{\boldsymbol{\varepsilon}}\dot{\tilde{\boldsymbol{\varepsilon}}} \quad (33)$$

| e-ISSN: 2278 – 8875, p-ISSN: 2320 – 3765| www.ijareeie.com | Impact Factor: 7.122|

||Volume 9, Issue 7, July 2020||

Therefore, using Eqs. (32) and (33), by applying Eq.(30) and the update rule for parameter $\hat{\varepsilon}$given by Eq.(15), the first-time derivative of the Lyapunov's functionis obtained as follows:

$$\dot{V} = \mathbf{tr}\left[\widetilde{\boldsymbol{W}}^T\left(\boldsymbol{\Gamma}\dot{\widehat{\boldsymbol{W}}} - \boldsymbol{h}(\boldsymbol{X_e})\right)\boldsymbol{s}^T\right] + \boldsymbol{s}^T\boldsymbol{\varepsilon}(\boldsymbol{X_e})\boldsymbol{I_2} + \boldsymbol{s}^T\boldsymbol{\xi_f}(\boldsymbol{t},\boldsymbol{u_i}) - \boldsymbol{s}^T\widehat{\boldsymbol{\eta}}\boldsymbol{T}(\boldsymbol{s}) - \boldsymbol{s}^T\boldsymbol{K}\boldsymbol{E}(\boldsymbol{s}) + \mathbf{tr}\left[\widetilde{\boldsymbol{\eta}}_1^T\boldsymbol{\Gamma}_\eta\dot{\widehat{\boldsymbol{\eta}}}_1\right] + \tilde{\boldsymbol{\varepsilon}}^T\boldsymbol{\Gamma}_\varepsilon\dot{\hat{\boldsymbol{\varepsilon}}}$$

$$= \boldsymbol{s}^T(\hat{\boldsymbol{\varepsilon}} - \tilde{\boldsymbol{\varepsilon}})\boldsymbol{I_2} + \boldsymbol{s}^T\boldsymbol{\xi_f}(\boldsymbol{t},\boldsymbol{u_i}) - \boldsymbol{s}^T\widehat{\boldsymbol{\eta}}\boldsymbol{T}(\boldsymbol{s}) - \boldsymbol{s}^T\boldsymbol{K}\boldsymbol{E}(\boldsymbol{s}) + \mathbf{tr}\left[\widetilde{\boldsymbol{\eta}}_1^T\boldsymbol{\Gamma}_\eta\dot{\widehat{\boldsymbol{\eta}}}_1\right] + \tilde{\boldsymbol{\varepsilon}}^T\boldsymbol{\Gamma}_\varepsilon\dot{\hat{\boldsymbol{\varepsilon}}} \quad (34)$$

$$= \boldsymbol{s}^T\boldsymbol{\xi_f}(\boldsymbol{t},\boldsymbol{u_i}) - \boldsymbol{s}^T\widehat{\boldsymbol{\eta}}\boldsymbol{T}(\boldsymbol{s}) - \boldsymbol{s}^T\boldsymbol{K}\boldsymbol{E}(\boldsymbol{s}) + \mathbf{tr}\left[\widetilde{\boldsymbol{\eta}}_1^T\boldsymbol{\Gamma}_\eta\dot{\widehat{\boldsymbol{\eta}}}_1\right] + \boldsymbol{s}^T\hat{\boldsymbol{\varepsilon}}\boldsymbol{I_2}$$

During the worst case corresponding to simultaneous perturbation severe perturbation causedby the lumped disturbance $\boldsymbol{\xi_f}(\boldsymbol{t},\boldsymbol{u_i})$ the variable $\mathbf{s}$ diverges fromthe origin such that $T_i(s_i) \cong 1$, and Eq. (34)can be rewritten as follows:

$$\dot{V} \cong \boldsymbol{s}^T\hat{\boldsymbol{\xi}}\boldsymbol{\xi_f}(\boldsymbol{t},\boldsymbol{u_i}) - \boldsymbol{s}^T\widehat{\boldsymbol{\eta}}\boldsymbol{I_2} - \boldsymbol{s}^T\boldsymbol{K}\boldsymbol{E}(\boldsymbol{s}) + \mathbf{tr}\left[\widetilde{\boldsymbol{\eta}}_1^T\boldsymbol{\Gamma}_\eta\dot{\widehat{\boldsymbol{\eta}}}_1\right] + \boldsymbol{s}^T\hat{\boldsymbol{\varepsilon}}\boldsymbol{I_2}$$

$$= \boldsymbol{s}^T(\widehat{\boldsymbol{\eta}}_1 - \widetilde{\boldsymbol{\eta}}_1)\boldsymbol{I_2} - \boldsymbol{s}^T(\widehat{\boldsymbol{\eta}}_1 + \boldsymbol{\eta}_2)\boldsymbol{I_2} - K_x\frac{s_x^2}{\exp(s_x)+1} - K_y\frac{s_y^2}{\exp(s_y)+1} + \mathbf{tr}\left[\widetilde{\boldsymbol{\eta}}_1^T\boldsymbol{\Gamma}_\eta\dot{\widehat{\boldsymbol{\eta}}}_1\right] + \boldsymbol{s}^T\hat{\boldsymbol{\varepsilon}}\boldsymbol{I_2} \quad (35)$$

$$= \boldsymbol{s}^T\widetilde{\boldsymbol{\eta}}_1\boldsymbol{I_2} - \boldsymbol{s}^T\boldsymbol{\eta}_2\boldsymbol{I_2} - K_x\frac{s_x^2}{\exp(s_x)+1} - K_y\frac{s_y^2}{\exp(s_y)+1} + \mathbf{tr}\left[\widetilde{\boldsymbol{\eta}}_1^T\boldsymbol{\Gamma}_\eta\dot{\widehat{\boldsymbol{\eta}}}_1\right] + \boldsymbol{s}^T\hat{\boldsymbol{\varepsilon}}\boldsymbol{I_2}$$

where $\hat{\eta}$and $\boldsymbol{\xi_f}(\boldsymbol{t},\boldsymbol{u_i})$are replaced by their expressionsgiven by Eqs. (12) and (28).

By applying the update rule$\dot{\hat{\eta}}_{1,j}$(with$j = x, y = 1, 2$) given by Eq. (13) in Eq. (35) we obtain:

$$\dot{V} = \mathbf{tr}\left[\widetilde{\boldsymbol{\eta}}_1^T\left(\boldsymbol{\Gamma}_\eta\dot{\widehat{\boldsymbol{\eta}}}_1 - \boldsymbol{I_2}\boldsymbol{s}^T\right)\right] - K_x\frac{s_x^2}{\exp(s_x)+1} - K_y\frac{s_y^2}{\exp(s_y)+1} + \boldsymbol{s}^T\hat{\boldsymbol{\varepsilon}}\boldsymbol{I_2} - \boldsymbol{s}^T\boldsymbol{\eta}_2\boldsymbol{I_2}$$

$$= \sum_{j=1}^{2}\left[\tilde{\eta}_{1,j}\left(\Gamma_{\eta,j}\dot{\hat{\eta}}_{1,j} - s_j\right)\right] - K_x\frac{s_x^2}{\exp(s_x)+1} - K_y\frac{s_y^2}{\exp(s_y)+1} + \boldsymbol{s}^T\hat{\boldsymbol{\varepsilon}}\boldsymbol{I_2} - \boldsymbol{s}^T\boldsymbol{\eta}_2\boldsymbol{I_2} \quad (36)$$

$$\leq \sum_{j=1}^{2}\left[|\tilde{\eta}_{1,j}|\left(\Gamma_{\eta,j}\dot{\hat{\eta}}_{1,j} - |s_j|\right)\right] - K_x\frac{s_x^2}{\exp(s_x)+1} - K_y\frac{s_y^2}{\exp(s_y)+1} + \boldsymbol{s}^T\hat{\boldsymbol{\varepsilon}}\boldsymbol{I_2} - \boldsymbol{s}^T\boldsymbol{\eta}_2\boldsymbol{I_2}$$

$$= -K_x\frac{s_x^2}{\exp(s_x)+1} - K_y\frac{s_y^2}{\exp(s_y)+1} + \boldsymbol{s}^T(\hat{\boldsymbol{\varepsilon}} - \boldsymbol{\eta}_2)\boldsymbol{I_2} \leq -K_x\frac{s_x^2}{\exp(s_x)+1} - K_y\frac{s_y^2}{\exp(s_y)+1} + \|\boldsymbol{s}\|(\|\hat{\boldsymbol{\varepsilon}}\| - \|\boldsymbol{\eta}_2\|)$$

By using $\boldsymbol{\eta_2}$for which the entries are given by Eq. (14) weobtain

$$\dot{V} \leq -K_x\frac{s_x^2}{\exp(s_x)+1} - K_y\frac{s_y^2}{\exp(s_y)+1} + \|\boldsymbol{s}\|\left(\frac{1}{\rho} - 1\right)\|\boldsymbol{\eta}_2\| \quad (37)$$

with $K_j > 0$ and $\rho > 1$, we have$\dot{V} \leq 0$. Therefore, theclosed-loop system is asymptotically stable despite uncertaindynamics, external disturbances and actuationfaults. Hence, we conclude that the control objective isachieved when theproposed NAFTNCis used with thedefined constant and dynamic parameters, as accordingto the Barbalat's lemma $\boldsymbol{e} \to \mathbf{0}$when$t \to \infty$.

V. SIMULATION AND DISCUSSION

In order to demonstrate the efficiency of the proposed NAFTNC in dealing simultaneously with external disturbances, uncertain parameters and actuation faults, in this section, simulation results of the controlled disturbed ducted fan, in Matlab/Simulink, are presented. Parameters of the simulated fan are as follows (Fazeli Asl & Seyyed, 2017): weight of fan $m_g = 0.46kg$, inertial mass in the x direction $m_x = 4.9kg$, inertial mass in the y direction $m_y = 8.5kg$, distance from the centre of mass $r = 0.12m$, moment of inertia $J = 0.05kgm^2$, viscous friction coefficient $d = 1.2Nms^{-1}$ and gravitational constant $g = 9.8ms^{-2}$.

The parameters for the RBFNN and the controller are selected as follows: $c_1 = c_2 = 5$, $K_1 = K_2 = 5$, $\gamma_{x\eta} = \gamma_{y\eta} = 15 \times 10^{-4}$, $\gamma_{\varepsilon x} = \gamma_{\varepsilon x} = 10 \times 10^{-3}$, $\rho = 2.5$, $\gamma_x = 0.8$, $\gamma_y = 0.5$, $\lambda_{xi} = \lambda_{yi} = [0.1 \quad 0.1]^T$ and $\beta_x = \beta_y = 0.5$.

To illustrate the highperformance of the proposed NAFTNC, its results are compared with those obtained using another nonlinear controller, which is atraditional sliding mode controller (SMC) designed as follows:

$$\boldsymbol{u_i} = \boldsymbol{K_a^{-1}}\left(-\boldsymbol{D}\boldsymbol{X_2} - \boldsymbol{m} + \ddot{\boldsymbol{X}}_{\boldsymbol{1d}} - \boldsymbol{c}\dot{\boldsymbol{e}} - \boldsymbol{\eta}\,\mathbf{sign}(\boldsymbol{s})\right) \quad (37)$$

where $\boldsymbol{s} = \dot{\boldsymbol{e}} + \boldsymbol{c}\boldsymbol{e}$ (with $\boldsymbol{c}$ being a diagonal matrix for which the entries are $c_1 = c_2 = 5$) and $\eta = 10$.The initial values of the fan's state variables are selected as: $[x_0 \quad y_0 \quad \theta_0] = [0.5 \quad 0.5 \quad -\pi/4]$.

| e-ISSN: 2278 – 8875, p-ISSN: 2320 – 3765| www.ijareeie.com | Impact Factor: 7.122|

||Volume 9, Issue 7, July 2020||

The simulation scenario is stated as follows: the desired trajectory is $x_d = \sin(t)$ and $y_d = 1.2\sin(2t)$. The external disturbances are as follows: $\boldsymbol{d_f} = [5\cos(t) \quad 5\cos(2t)]^T$. We consider that at simulation time $t \geq 10sec$ the actuator loses 50% of its effectiveness and that at simulation time $t \geq 20sec$ there is a 10% increase in the values of parameters m_g, m_x,m_y, r, J, and d. Figures 2, 3 and 4 depict simulation results of the ducted fan system controlled by the proposed NAFTNCand by the SMC under the aforementioned perturbations.

Figures 2(a) and (b) show the fan's x position tracking its desired value x_d and the tracking error e_x, respectively; x_{NAFTNC} is the x position obtained using the NAFTNC while x_{smc} is the one obtained using the traditional SMC.

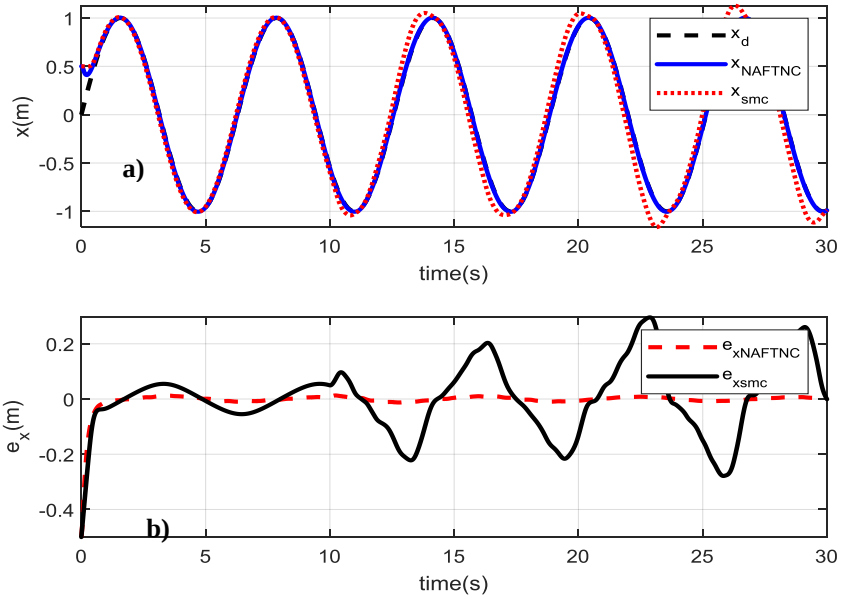

Figure 2. a) x position obtained using the NAFTNC and the SMC tracking its desired value x_d; b) tracking error on x when the NAFTNC and the SMC are used, respectively.

Figures 3(a) and (b) depict the fan's y position tracking its desired value y_d and the tracking error e_y, respectively; y_{NAFTNC} is the y position obtained using the NAFTNC while y_{smc} is the one obtained using the traditional SMC.

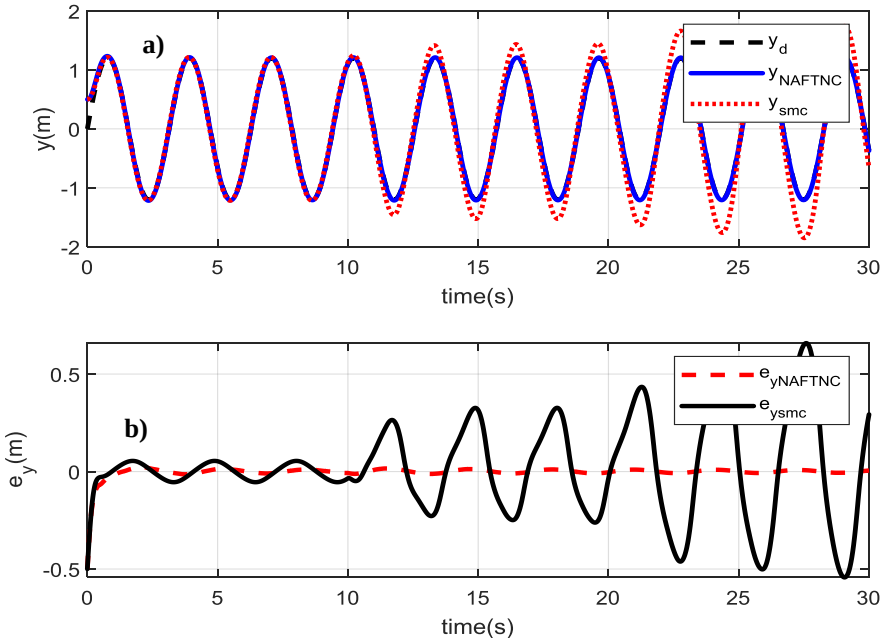

Figure 3. a) y position obtained using the NAFTNC and the SMC tracking its desired value y_d; b) tracking error on y when the NAFTNC and the SMC are used, respectively.

| e-ISSN: 2278 – 8875, p-ISSN: 2320 – 3765| www.ijareeie.com | Impact Factor: 7.122|

||Volume 9, Issue 7, July 2020||

Figures 2 b) and 3 b) show that, at simulation times $t = 10sec$ and $t = 20sec$, when a 50% loss of effectiveness and a 10% increase in fan's parameters values occur, respectively, errors on$x$ and y positions increase considerably when the SMC is applied. However, these figures illustrate how a higher performance is achieved when the NAFTNC is applied is these adverse conditions, as tracking errors on x and y remain very close to zero. The control signals u_x and u_y leading to results depicted in Figs. 2 and 3 are illustrated in Figs.4 and 5 for the NAFTNC and the SMC, respectively. As one can observe, these signals are both continuous, which is good for practical applications. It is also obvious that the control signals obtained using the NAFTNC, which yields very good performance, remain bounded as $-120.8N \leq u_{xNAFTNC} \leq 114.7N$ and $-131N \leq u_{yNAFTNC} \leq 51N$)while the one obtained using the SMC are bounded as$-142.5N \leq u_{xSMC} \leq 139.4N$ and $-132N \leq u_{ySMC} \leq 136N$. In fact, the difference between control signals obtained using the two controllers is not too obvious while the results they correspond to in terms of tracking errors are too different. Hence, the ducted fan aircraft using the proposed NAFTNC is able to perform its mission with high performance in spite adverse conditions.

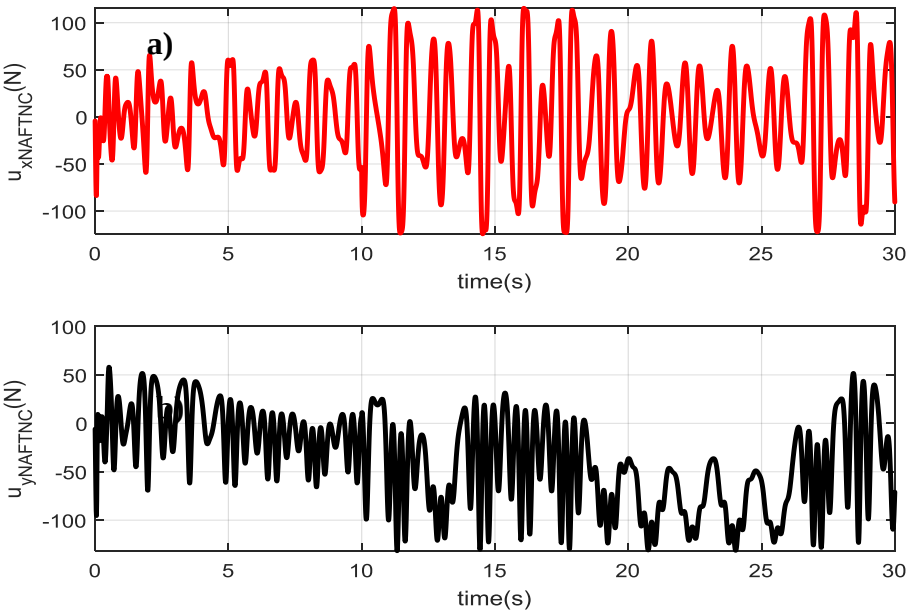

Figure 4. a) Control signal u_x provided by the NAFTNC; b) Control signal u_y provided by the NAFTNC.

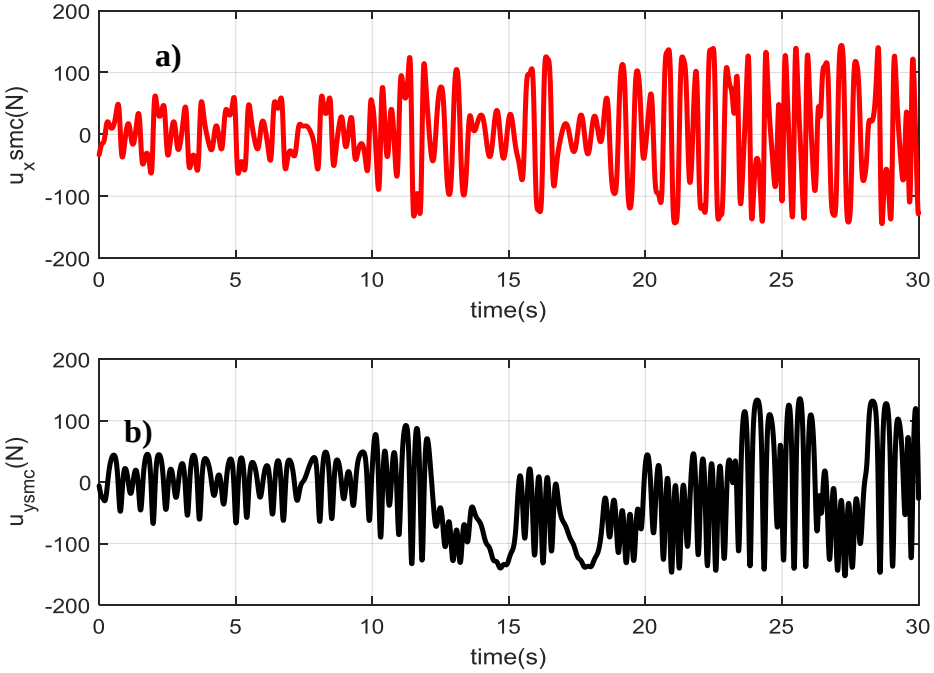

Figure 5. a) Control signal u_x provided by the SMC; b) Control signal u_y provided by the SMC

| e-ISSN: 2278 – 8875, p-ISSN: 2320 – 3765| www.ijareeie.com | Impact Factor: 7.122|

||Volume 9, Issue 7, July 2020||

VI.CONCLUSION

This paper has addressed the control problem of a ducted fan subject, simultaneously, to external disturbances, uncertain dynamics and actuation failure. An adaptive nonlinear controller has been designed using some dynamic parameters and two radial basis function neural networks to tackle the aforementioned disturbances. Through a stability analysis, the proposed controller has been proved to be able to guarantee the closed-loop system stability despite severe conditions corresponding to external disturbances, loss of effectiveness actuator's fault and unpredicted parameter changes. This good performance has been demonstrated also by simulatingthe ducted fan with Matlab/Simulink. It has been demonstrated that with the proposed adaptive nonlinear controller, a higher performance is achieved when compared to the one obtained using another nonlinear control approach, which is the sliding mode control. Hence, the use of the proposed control enables the achievement of high performance to the ducted fan aircraft despite some adverse condition

REFERENCES

[1] S. Fazeli Asl and M. S. Seyyed, "Adaptive Backstepping Fast Terminal Sliding Mode Controller Design for Ducted Fan Engine of Thrust-Vectored Aircraft," Aerospace Science and Technology, 2017.
[2] A. Jadbabaie and J. Hauser, "Control of a thrustĞvectored flying wing: a receding horizon—LPV approach," International Journal of Robust and Nonlinear, vol. 12, no. 9, pp. 869-896, 2002.
[3] S. Deng, S. Wang and Z. Zhang, "Aerodynamic performance assessment of a ducted fan UAV for VTOL applications," Aerosp. Sci. Technol., 2020.
[4] S. Emami and Rezaeizadeh, "Adaptive model predictive control-based attitude and trajectory tracking of a VTOL attitude and trajectory tracking of a VTOL," IET Control Theory & Applications, p. 12, 2018.
[5] J. Chen, G. Huang and X. Xiang, "Numerical investigations of ducted fan aerodynamic performance with tip-jet," Aerospace Science and Technology, vol. 78, pp. 510-521, 2018.
[6] Z. Cheng, H. Pei and S. Li, "Neural-Networks control for hover to high-speed-level-flight transition of ducted fan UAV with provable stability," IEEEE Access, vol. 8, p. 17, 2020.
[7] M. Muehlebach and R. D'Andrea, "The Flying Platform – A testbed for ducted fan actuation and control design," Mechatronics, vol. 42, pp. 52-68, 2017.
[8] R. Naldi, A. Torre and L. Marconi, "Robust Control of a Miniature Ducted-Fan Aerial Robot for Blind Navigation in Unknown Populated Environments," IEEE TRANSACTIONS ON CONTROL SYSTEMS TECHNOLOGY, vol. 23, no. 1, pp. 64-79, 2015.
[9] I. Peddle, T. Jones and J. Treurnicht, "Practical near hover flight control of a ducted fan (SLADe)," Control Engineering Practice, vol. 17, pp. 48-58, 2009.
[10] M. Muehlebach and R. D'Andrea, "The Flying Platform – A testbed for ducted fan actuation and control design," Mechatronics, vol. 42, pp. 52-68, 2017.
[11] X. Wang, C. Xiang, H. Najjaran and B. Xu, "Robust adaptive fault-tolerant control of a tandem coaxial ducted fan aircraft with actuator saturation," Chinese Journal of Aeronautics, 2018.
[12] J. Yu, A. Jadbabaie and Primbs, "Comparison of nonlinear control design techniques on a model of the Caltech ducted fan," Automatica, vol. 37, pp. 1971-1978, 2001.
[13] J. Yu, A. Jadbabaie and J. H. Y. Primbs, "Comparison of nonlinear control designs for a ducted fan model," in 14th Trienial World Congress, Beijing, P.R. China, 1999.
[14] T. Cimen, "Approximate nonlinear optimal SDRE tracking control," in 17th IFAC Aerospace Symposium on Automatic Control, 2007.
[15] X. Wang, J. Liu and K.-Y. Cai, "Tracking control for VTOL aircraft with disabled IMUs," International Journal of Systems Science, vol. 41, no. 10, 2010.
[16] W. Lili, S. Yixin, Z. Huajun, T. Yongchuan and S. Binghua, "Neural adaptive sliding mode controller for unmanned surface vehicle steering system," Advances in mechanical engineering, vol. 10, no. 9, pp. 1-12, 2018.
[17] M. Dongdong, W. Guofeng, F. Yunsheng, B. Yiming and Z. Yongsheng, "Fuzzy-Based Optimal Adaptive Line-of-Sight Path Following for Underactuated Unmanned Surface Vehicle with Uncertainties and Time-Varying Disturbances," Hindawi Mathematical Problems in Engineering, vol. 2018, p. 12, 2018.